

Research Paper

Analyzing the Data of Galaxies in Different Scales Using Wavelet Transform

Aria Hemmatian^{*1} · Reza Rezaei²

¹ Department of Physics, Sharif University of Technology, Tehran, Iran;

*E-mail: ariahemmatian81@gmail.com

² Department of Physics, Sharif University of Technology, Tehran, Iran;

E-mail: reza.rezaei@sharif.edu

Received: 15 December 2025; **Accepted:** 27 December 2025; **Published:** 29 December 2025

Abstract. One of the methods used to analyze the data obtained from a galaxy is to examine it in different scales. The data usually consists of many different wavelengths, and analyzing the structures of the same size in these images can be extremely insightful [1–3]. Fortunately, a potent mathematical tool called wavelet exists for this exact purpose. Using wavelet analysis, we can decompose an image into structures of different scales, called the wavelet coefficients. Further investigations can be accomplished using wavelet spectrum and scale cross-correlations, which help us understand the energy distribution in scales. In this paper, we utilize the methods of wavelet scale analysis on the data from the galaxies M74 and DDO 69 to extract valuable information from them.

Keywords: Wavelet Transform, PetHat Wavelet, Scale Cross-Correlation, Data Analysis, M74, DDO69.

1 Introduction

Wavelet Transform is one of the most useful image processing tools that can be used for removing noise and hot pixels from images, find the edges in an image and finding scales of structures in an image. The last use mentioned can be utilized for astrophysical scale-dependent analysis of galaxies. In order to use continuous wavelet transform in our analysis we wrote a Python script, and the some of the results from the script are mentioned in this paper, but first we'll explain the theoretical basis of wavelet transforms.

2 Wavelet Transforms for Scale-dependent Analysis

Wavelet transform of data is a convolution of data with a wavelet to separate it into different scales. Wavelets are local functions of position and scale, which means that wavelet transform is an extension of Fourier transform. Harmonic functions are used in Fourier transforms, whereas wavelets are localized functions that go to zero rapidly.[1,3] Suppose

**Corresponding author*

This is an open access article under the **CC BY** license.



that $\psi(\mathbf{x})$ is a wavelet. Then, the wavelet coefficient of a function $f(\mathbf{x})$ in scale a is given by [1]

$$W(a, \mathbf{x}) = \frac{1}{a^2} \int_{\mathbb{R}^2} f(\mathbf{x}') \psi\left(\frac{\mathbf{x} - \mathbf{x}'}{a}\right) d\mathbf{x}'. \quad (1)$$

To simplify this, and for ease and speed of computation, we'll go to the Fourier space. Therefore, [1]

$$W(a, \mathbf{x}) = \frac{1}{4\pi^2} \int_{\mathbb{R}^2} \hat{f}(\mathbf{k}) \hat{\psi}(a\mathbf{k}) e^{i\mathbf{k} \cdot \mathbf{x}} d\mathbf{k}, \quad (2)$$

where \mathbf{k} is the Fourier conjugate of \mathbf{x} . Consequently, calculating wavelet coefficient goes from computing a 2D convolution to three 2D Fourier transform. Additionally, due to the fact that astronomical data is a discrete sample of the intensity distribution of the target, the Fourier transforms in equation 2 becomes discrete ($f(\mathbf{x})$ contains a dirac comb). As a result, we can use the FFT algorithm (time complexity $\mathcal{O}(n^2 \log n)$) which means that computing equation 2 is much faster than equation 1 which has a time complexity of $\mathcal{O}(n^4)$. The distribution of structures of different scales can be calculated from wavelet spectrum, defined as [1]

$$M(a) = \int_{\mathbb{R}^2} |W(a, \mathbf{x})|^2 d\mathbf{x} = \frac{1}{16\pi^2} \int_{\mathbb{R}^2} |\hat{f}(\mathbf{k})|^2 |\hat{\psi}(a\mathbf{k})|^2 d\mathbf{k}, \quad (3)$$

the value of the wavelet spectrum indicates the number of structures in each scale[1]. Finally, the scale cross-correlation of two different maps in scale a is given by

$$r_W(a) = \frac{\int \int W_1(a, \mathbf{x}) W_2^*(a, \mathbf{x}) d\mathbf{x}}{\sqrt{M_1(a) M_2(a)}}, \quad (4)$$

and the error of the correlation is given by

$$\Delta r_W(a) = \frac{\sqrt{1 - r_W^2(a)}}{\sqrt{\frac{L^2}{a^2} - 1}}, \quad (5)$$

where L is the size of the map. Using this equation, we can calculate the scale-dependent cross-correlation of a galaxies map in two different filters.

In this paper, we use the *PetHat* wavelet that is an isotropic function and has a relatively decent spectral resolution [1,4]. This makes it a suitable wavelet for our purposes. It is defined by its Fourier transform

$$\hat{\psi}(\mathbf{k}) = \begin{cases} \cos^2\left(\frac{\pi}{2} \log_2 \frac{|\mathbf{k}|}{2\pi}\right), & \pi < |\mathbf{k}| < 4\pi, \\ 0, & \text{otherwise.} \end{cases} \quad (6)$$

The radial graph of this wavelet is given in Figure 1.

3 Results

Firstly, we analyzed the map of M74 galaxy (spiral and face-on) in filter g taken by the PS1 survey [5]. Some of the coefficients are plotted in Figure 2. As it is evident in the coefficients, HII regions are detected at the 5 arcsec scale and at the higher scales, the spiral arms of the galaxy are detected as well. Lastly, M74's core is detected at the largest scale.

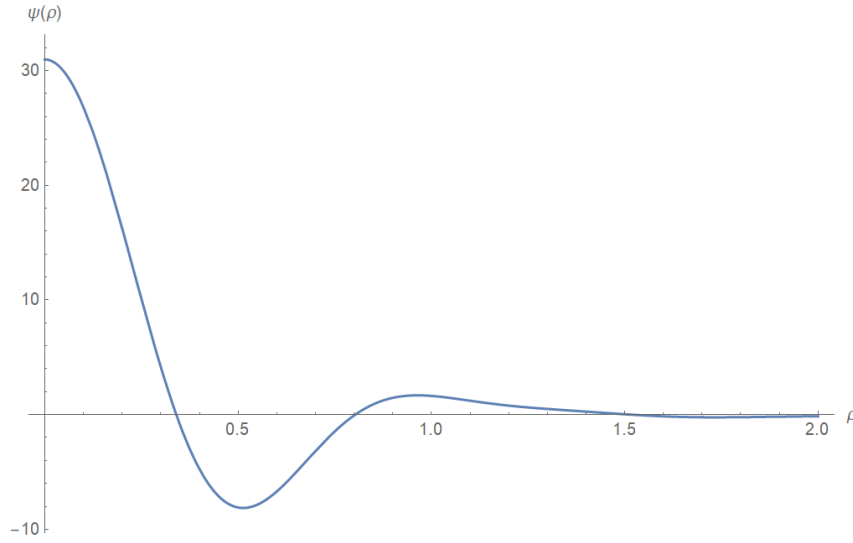


Figure 1: PetHat wavelet as a function of radial distance. This wavelet is isotropic and as a result only a function of radial distance.

The same analysis was done for the DDO69 dwarf galaxy (irregular, in Leo constellation) taken by the LITTLETHINGS survey [6]. Wavelet coefficients of the visible map are shown in Figure 3. Moreover, the wavelet spectrum of this galaxy in the B and V filters is shown in Figure 4. Finally the wavelet cross-correlation of the maps of this galaxy in V and B filters is plotted in Figure 5.

Although the intensity of the galaxy in these filters is similar to each other, we can see in Figures 4 and 5 that the radiation of this galaxy in these filters has slight differences in small scale structures. The normal cross-correlation of these maps is 0.9834 ± 0.0005 , which means that scale cross-correlation contains a lot more information compared to the normal cross-correlation.

4 Discussion

Wavelet's scale cross-correlation is extremely useful in the analysis of correlation between two structures. For example, if two maps are highly correlated in large scales and highly anti-correlated in small scales, then the overall cross correlation would be close to zero. However, scale cross-correlation is sensitive to correlation at different scales and as a result, such analysis would be more meaningful using that tool. In this example, wavelet cross-correlation would correctly detect a negative correlation in small scales and a positive correlation in large scales [7] and therefore, would provide a more comprehensive result compared to a normal cross-correlation.

As it is evident from the results, wavelet transform can be used for extracting significant information regarding scales of different size from actual astronomical data as well. For example, in Figure 2, HII regions (5 arcsec), spiral arms (20 to 80 arcsec) and the core (150 arcsec) of M74 affect the wavelet coefficient in different scales, which couldn't be analyzed deeply using Fourier analysis. Similarly, the spectrum of these two maps is more or less aligned, which means that the radiation of DDO69 in these two filters are originates from the same structures. Finally, the slow-scale differences of DDO69 in B and V filters become

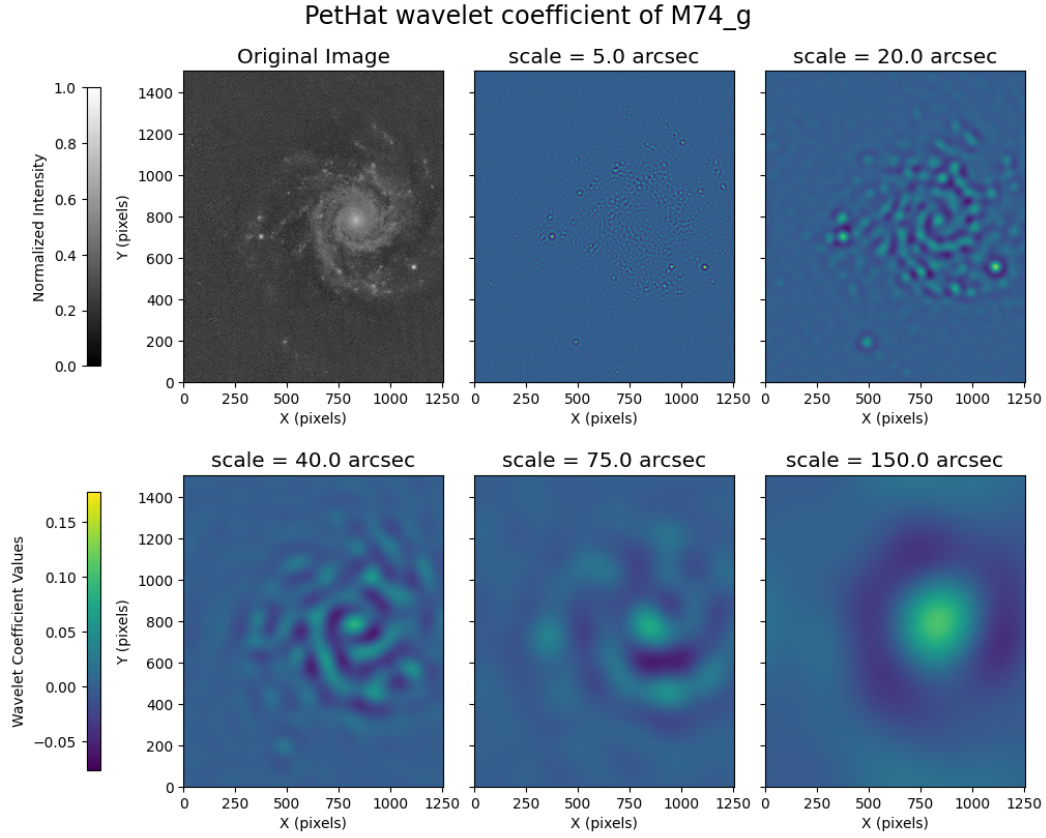


Figure 2: Wavelet coefficients of M74. This image is $11' \times 12'$. The main map is in grayscale and normalized to one. The other maps are the wavelet coefficients of the original image in 5 different scales. HII regions and spiral arms of M74 has been detected by the wavelet coefficients.

evident in the cross-correlation of these two maps (Figure 5) as it is below 0.8 in scales below 20 arcsec.

Lastly, it is important to note that in order to avoid oversampling, one can't use wavelet analysis over a continuous range of scales, despite the wavelet transform itself being continuous. In case of the PetHat wavelet, the optimal scales are powers of two [7], and for using this tool in scientific analysis this criteria must be satisfied.

In short, this tool has a lot of uses in astronomical image processing (e.g. analyzing H_α radiation only in the scales of the HII regions or denoising an astronomical image), specially the continuous wavelet transform that we used. We are hoping to use our Python script to conduct scientific analysis on data and extract information that is not possible to find from customary means.

Authors' Contributions

All authors have the same contribution.

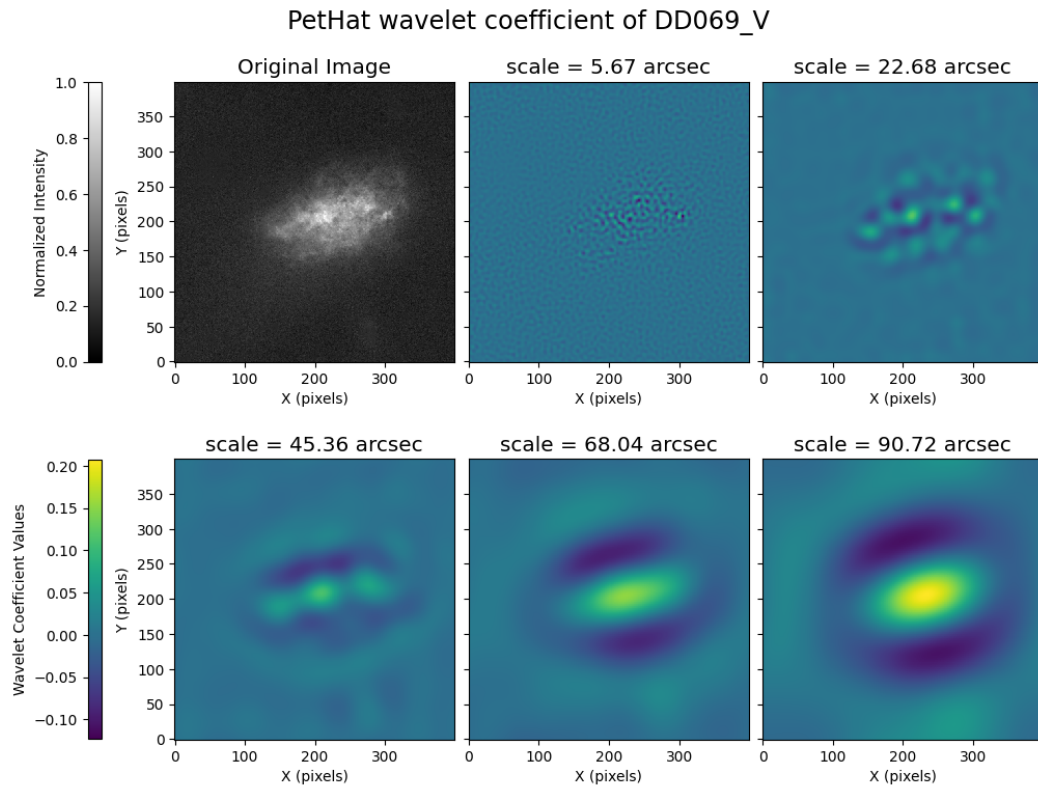


Figure 3: Wavelet coefficients of DDO69. This image is $8' \times 8'$. The main map is in grayscale and normalized to one. The other maps are the wavelet coefficients of the original image in 5 different scales.

Data Availability

No data available.

Conflicts of Interest

The authors declare that there is no conflict of interest.

Ethical Considerations

The authors have diligently addressed ethical concerns, such as informed consent, plagiarism, data fabrication, misconduct, falsification, double publication, redundancy, submission, and other related matters.

Funding

This research did not receive any grant from funding agencies in the public, commercial, or nonprofit sectors.

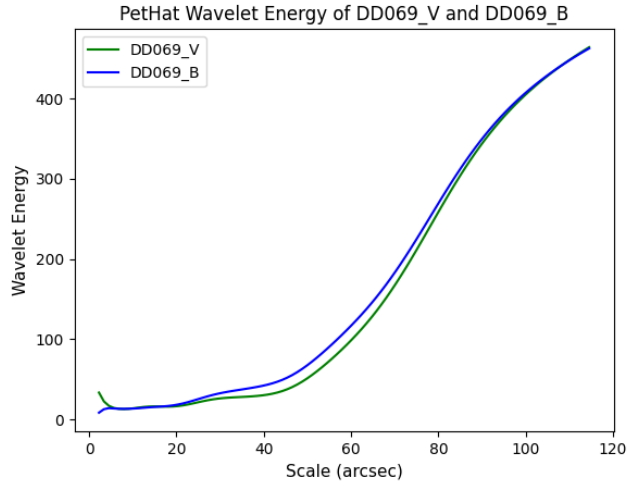


Figure 4: Wavelet Spectrum of DDO69 in V and B filters. The spectrum of these two maps are more or less aligned, which means that the radiation of DDO69 in these two filters are originated from the same structures.

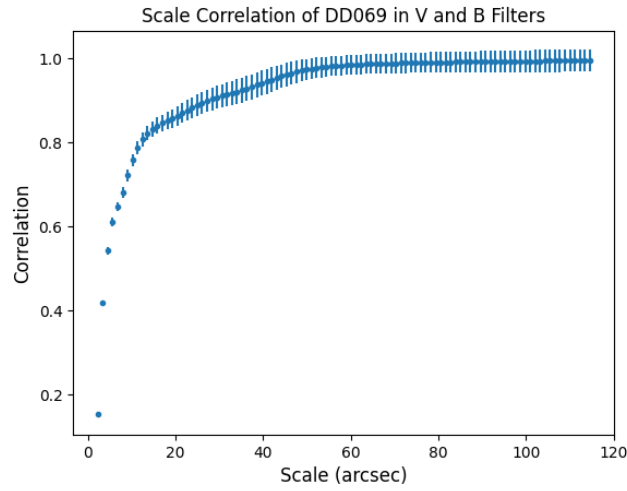


Figure 5: Wavelet Cross-correlation of DDO69 in V and B filters. This method provides a more thorough analysis compared to a normal cross-correlation.

References

- [1] Frick, P., Beck, R., Berkhuijsen, E., & Patrickeyev, I. 2001, MNRAS, 327, 1145.
- [2] Keilmann, E., et al. 2024, A&AS, 692, A226.
- [3] Holschneider, M. Wavelets - an analysis tool, 2021.
- [4] Aurell, E., Frick, P., & Shaidurov, V. 2002, Physica D: Nonlinear Phenomena, 72, 95.
- [5] Chambers, K. C., et al. The Pan-STARRS1 Surveys, 2016.

- [6] Hunter, D. A., et al. 2012, AJ, 144, 134.
- [7] Tabatabaei, F. S., et al. 2013, A&A, 557, A129.